Inorg. Chem. **2000,** *39,* 4107−4112

Hydrolysis, Hydrosulfidolysis, and Aminolysis of Imido(methyl)rhenium Complexes

Wei-Dong Wang, Ilia A. Guzei, and James H. Espenson*

Ames Laboratory and Department of Chemistry, Iowa State University of Science and Technology, Ames, Iowa 50011

Received January 31, 2000

The tris(imido)methylrhenium complex $CH_3Re(NAd)_3$ (**1a**, Ad = 1-adamantyl) reacts with H_2O to give $CH_3Re(NAd)_2O$ (**2a**) and $AdNH_2$. The resulting di(imido)oxo species can further react with another molecule of H_2O to generate $CH_3Re(NAd)O_2$ (**3a**). The kinetics of these reactions have been studied by means of ^1H NMR and UV−vis spectroscopies. The second-order rate constant for the reaction of **1a** with H_2O at 298 K in C_6H_6 is 3.3 L mol^{-1} s^{-1}, which is much larger than the value 1×10^{-4} L mol^{-1} s^{-1} obtained for the reaction between $CH_3Re(NAr)_3$ (**1b**, Ar = 2,6-diisopropylphenyl) and H_2O in CH_3CN at 313 K. Both **1a** and **1b** react with H_2S to produce the rhenium(VII) sulfide, $\{CH_3Re(NR)_2\}_2(\mu\text{-S})_2$ (**4a**, R = Ad; **4b**, R = Ar), with second-order rate constants of 17 and 1.6×10^{-4} L mol^{-1} s^{-1} in C_6H_6 and CH_3CN, respectively. Complex **4b** has been structurally characterized. The crystal data are as follows: space group $C2/c$, $a = 30.4831$ (19) Å, $b = 10.9766$ (7) Å, $c = 18.1645$ (11) Å, $\beta = 108.268(1)°$, $V = 5771.5$ (6) Å^3, $Z = 4$. The reaction between $CH_3Re(NAr)_2O$ (**2b**) and H_2S also yields the dinuclear compound **4b**. Unlike **1b**, **1a** reacts with aniline derivatives to give mixed imido rhenium complexes.

Introduction

Transition-metal imido complexes are believed to be the active intermediates in nitrene transfer reactions.[1,2] Their relevance in manufacturing of acrylonitrile, organic syntheses, and nitrogen fixation are well established.[3,4] A number of examples of metal−imido complexes undergoing hydrolysis, aminolysis, and hydrosulfidolysis have been reported.[5,6] In some cases, these reactions have been used to prepare new oxo, imido, and sulfido complexes.[7] Except for the in-depth investigation of the imido/amine exchange reaction,[8] detailed kinetic and mechanistic studies have not been carried out to compare the reactivity of different imido moieties toward different nucleophiles. In the course of investigating the nitrene (NR) transfer reaction, we studied the reactivity of imido(methyl)rhenium complexes toward water, hydrogen sulfide, and amines. Here we would like to report a remarkable difference in reactivity between arylimido and alkylimido rhenium(VII) complexes toward hydrolysis, hydrosulfidolysis, and aminolysis.

Experimental Section

Materials. Aniline derivatives and hydrogen sulfide used for this work were purchased from Aldrich and used as received, except 4-methoxyaniline, which was recrystallized before being used. High-purity water was obtained by passing laboratory-distilled water through a Millipore-Q water purification system. Toluene (Fisher), benzene-d_6 (CIL), and hexane (Fisher) were dried with sodium/benzophenone and stored in a nitrogen-filled glovebox. Other solvents, such as anhydrous CH_3CN (Aldrich) and CD_3CN (CIL), were used as received. Methylrhenium trioxide,[9] $CH_3Re(NAd)_3$ (**1a**, Ad = 1-adamantyl),[10] $CH_3Re(NAr)_3$ (**1b**, Ar = 2,6-diisopropylphenyl), and $CH_3Re(NAr)_2O$ (**2b**) were prepared according to the literature procedures.[11] Table 1 presents UV−vis and NMR data for the various rhenium compounds used in this study.

Table 1. NMR and Optical Parameters of the Imido(methyl)rhenium Complexes[a] in C_6D_6

compound	NMR ^1H, δ/ppm	NMR ^{13}C, δ/ppm	UV−vis λ_{max}/nm (ϵ/L mol^{-1} cm^{-1})
$CH_3Re(NAd)_3$	1.99	−6.5	375 (640 ± 30)
$CH_3Re(NAd)_2O$	1.91	0.80	
$CH_3Re(NAd)O_2$	1.75	8.1	355 (580 ± 30)
CH_3ReO_3	1.21	17.4	
$\{CH_3Re(NAd)_2\}_2(\mu\text{-S})_2$	2.03	3.9	525 (440 ± 20)
$CH_3Re(NAr)_3$	2.73	9.2	481 (4730 ± 20)[b]
$CH_3Re(NAr)_2O$	2.29	10.5	424 (7210 ± 70)[b]
$CH_3Re(NAr)O_2$	1.88	11.9	
$\{CH_3Re(NAr)_2\}_2(\mu\text{-S})_2$	2.40	13.8	575 (3040 ± 20)[b]

[a] Ad = 1-adamantyl; Ar = 2,6-diisopropylphenyl. [b] In CH_3CN.

Kinetic Studies. The stock solution of **1a** in C_6H_6 was prepared and stored in a glovebox. The concentration of water in a water-saturated benzene solution is 35 mM,[12] while the concentrations of hydrogen sulfide in its saturated benzene and acetonitrile solutions are 0.41 and 0.95 M, respectively.[13] The saturated hydrogen sulfide

---

(1) Mansuy, D.; Mahy, J. P. In *Metalloporphyrins Catalyzed Oxidations*; Monatnari, F., Casella, L., Eds.; Kluwer Academic Publishers: Dordrecht, 1994; p 175 and references therein.

(2) Au, S.-M.; Huang, J.-S.; Yu, W.-Y.; Fung, W.-H.; Che, C.-M. *J. Am. Chem. Soc.* **1999**, *121*, 9120.

(3) Nugent, W. A.; Mayer, J. M. *Metal-Ligand Multiple Bonds*; John Wiley & Sons: New York, 1988.

(4) Wigley, D. E. *Prog. Inorg. Chem.* **1994**, *42*, 239.

(5) Swallow, D.; McInnes, J. M.; Mountford, P. *J. Chem. Soc., Dalton Trans.* **1998**, 2253.

(6) Howard, W. A.; Trnka, T. M.; Waters, M.; Parkin, G. *J. Organomet. Chem.* **1997**, *528*, 95.

(7) Parkin, G. *Prog. Inorg. Chem.* **1998**, *47*, 1.

(8) Michelman, R. I.; Bergman, R. G.; Andersen, R. A. *Organometallics* **1993**, *12*, 2741.

(9) Herrmann, W. A.; Kratzer, R. M.; Fischer, R. W. *Angew. Chem., Int. Ed. Engl.* **1997**, *36*, 2652.

(10) Wang, W.-D.; Espenson, J. H. *Organometallics* **1999**, *18*, 5170.

(11) Herrmann, W. A.; Ding, H.; Kühn, F. E.; Scherer, W. *Organometallics* **1998**, *17*, 2751.

(12) Kirchnerova, J.; Cave, G. C. B. *Can. J. Chem.* **1976**, *54*, 3909.

(13) Fogg, P. G. T.; Gerrard, W. *Solubility of Gases in Liquids*; John Wiley & Sons: Chichester, 1991.

10.1021/ic0000956 CCC: $19.00

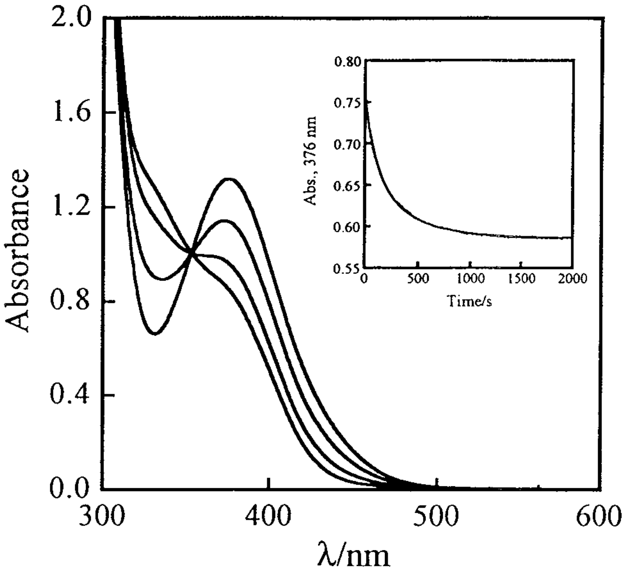

Figure 1. UV−vis titration of the hydrolysis reaction between 2.0 mM $CH_3Re(NAd)_3$ (Ad = 1-adamantyl) and H_2O in C_6H_6 at 298 K. The inset shows the kinetic trace at 375 nm for the reaction between 1.2 mM $CH_3Re(NAd)_3$ and 1.7 mM H_2O in C_6H_6 at 298 K. The clean isosbestic point signals the single reaction that forms $CH_3Re(NAd)_2O$.

solutions were prepared by purging H_2S through the benzene or acetonitrile solutions for at least 30 min. Variation of purging time from 30 to 50 min gave similar kinetic results, indicating that the saturation has been reached in 30 min.

Unless otherwise stated, kinetics experiments were carried out at 298 K by the use of a Shimadzu UV 3101PC or a Shimadzu MultiSpec 1500 equipped with a cell holder to control temperature thermoelectrically. The reactions of **1a** with H_2O and H_2S were studied under second-order conditions. The absorbance−time data were fitted to the following equation:[14]

$$\mathrm{Abs}_t = \frac{\mathrm{Abs}_\infty + \left\{\mathrm{Abs}_0\left(1 - \frac{[\mathrm{A}]_0}{[\mathrm{B}]_0}\right) - \mathrm{Abs}_\infty\right\}\exp(-k\Delta_0 t)}{1 - \frac{[\mathrm{A}]_0}{[\mathrm{B}]_0}\exp(-k\Delta_0 t)}$$

where $\Delta_0 = [B]_0 - [A]_0$. For the hydrolysis of **1a** in C_6H_6, the absorbance decrease at 375 nm was followed, Figure 1. Five experiments with the ratios of $[\mathbf{1a}]_0/[H_2O]_0$ ranging from 2.6 to 0.64 were performed ($[\mathbf{1a}]_0 = 0.47{-}2.0$ mM; $[H_2O]_0 = 0.74{-}1.7$ mM). The fit of the data in each experiment to the integrated rate equation and the constancy of the value of *k* obtained over the concentrations used were used to establish that the reaction does follow second-order rate law. The rate constant in C_6H_6 at 298 K is 3.3 ± 0.8 L mol^{-1} s^{-1}. The hydrolysis of $CH_3Re(NAd)_2O$ (**2a**) in C_6D_6 was studied by ^1H NMR. The methyl resonances were monitored for the consumption of **2a** and the formation of $CH_3Re(NAd)O_2$ (**3a**). A second-order rate constant of (9 ± 1) × 10^{-3} L mol^{-1} s^{-1} was obtained. For the hydrosulfidolysis of **1a**, the formation of $\{CH_3Re(NAd)_2\}_2(\mu\text{-}S)_2$ (**4a**) was monitored at 525 nm. The ratio of $[\mathbf{1a}]_0/[H_2S]_0$ in six experiments was varied from 3.7 to 0.18 ($[\mathbf{1a}]_0 = 0.35{-}1.8$ mM, $[H_2S]_0 = 0.49{-}2.5$ mM), and the second-order rate constant was 17 ± 2 L mol^{-1} s^{-1}. The formation of **4a** from the reaction of **2a** and H_2S in C_6H_6 was studied with **2a** in excess, and a rate constant of 95 ± 10 L mol^{-1} s^{-1} was obtained. The reaction of **1a** (1.8 mM) and $2,6\text{-}Me_2C_6H_4NH_2$ ($Ar'NH_2$, 27 mM) took place with a second-order rate constant of (1.6 ± 0.2) × 10^{-3} L mol^{-1} s^{-1} in C_6H_6 at 298 K.

The hydrolysis and hydrosulfidolysis of **1b** were studied by the initial rate method. The absorbance−time profile for the first 5% of the reaction was followed. For the hydrolysis of **1b** in CH_3CN at 40 °C, the absorbance change at 481 nm was monitored. The molar absorptivity for **1b** at 481 nm (an absorption maximum) is $\epsilon = 4730 \pm 20$ L mol^{-1} cm^{-1}, while $\epsilon = 3220$ L mol^{-1} cm^{-1} applies for **2b** at this wavelength. A second-order rate constant of (1.0 ± 0.2) × 10^{-4} L mol^{-1} s^{-1} was obtained. Similarly, the hydrolysis of **2b** was studied in CH_3CN at 40 °C. The initial rate, obtained by following the absorbance change at 443 nm ($\Delta\epsilon = 2400$ L mol^{-1} cm^{-1}), was proportional to the concentrations of water, which were varied from 1.7 to 16 M. A second-order rate constant of (4 ± 1) × 10^{-6} L mol^{-1} s^{-1} was obtained. The initial rates for the reaction of **1b** and H_2S in CH_3CN at 25 °C are proportional to the concentrations of **1b** (0.021−0.13 mM) and H_2S (0.15−0.70 M). Using the value of 3040 L mol^{-1} cm^{-1} for $\Delta\epsilon$ at 575 nm, a second-order rate constant of (1.6 ± 0.3) × 10^{-4} L mol^{-1} s^{-1} was obtained.

The hydrosulfidolysis of **2b** in CH_3CN was studied in the presence of 41 mM H_2O. The effect of H_2S, varying from 18 to 110 mM, was investigated at 2.4 mM $Ar'NH_2$ and 0.054 mM **2b**. The effect of **2b**, varying from 0.027 to 0.11 mM, was studied at 1.4 mM $Ar'NH_2$ and 36 mM H_2S. The formation of **4b** is first-order with respect to **2b** and H_2S. The effect of $Ar'NH_2$, varying from 0 to 1.4 mM, was studied at 0.054 mM **2b** and 36 mM H_2S, Figure S1. The reaction scheme consisting of eqs 4−6 was simulated using the Kinsim program.[15] The rate constants obtained from the simulated data are linearly proportional to the concentration of $Ar'NH_2$.

Preparation of $\{CH_3Re(NR)_2\}_2(\mu\text{-}S)_2$ (4). Complex **4b** (R = Ar) was prepared by injecting 6 mL of H_2S gas into a 10 mL hexane solution of 100 mg of **2b** (0.176 mmol). After 1 h, most of the hexane was removed by vacuum. The concentrated solution was then cooled to −20 °C, and dark red sheet crystals (55 mg, 53% yield) were obtained. ^1H NMR (C_6D_6): 1.11 (d, *J* = 6.8 Hz, 12H), 1.14 (d, *J* = 6.8 Hz, 12H), 2.40 (s, 3H), 3.59 (septet, *J* = 6.8 Hz, 4H), 7.02 (s, 6H). ^{13}C NMR (C_6D_6): 13.77 ($\mathbf{C}H_3Re$), 23.56 ($CH(\mathbf{C}H_3)_2$), 23.83 ($CH(\mathbf{C}H_3)_2$), 29.24 ($\mathbf{C}H(CH_3)_2$), 123.29, 142.30, 147.31. ES MS: MH_2^{2+}, 585; M^+, 1168. Anal. Found: C, 51.69; H, 6.57; N, 4.81; S, 5.66. Calcd for $C_{50}H_{74}N_4Re_2S_2$ (fw = 1167.75): C, 51.43; H, 6.39; N, 4.80; S, 5.49. The absorbance of **4b** at 575 nm in benzene ($\epsilon_{575\,nm} = 3040 \pm 20$ L mol^{-1} cm^{-1}) linearly increases as the concentration changes from 2 × 10^{-5} mol L^{-1} to 1 × 10^{-3} mol L^{-1}, Figure S2. Compound **4a** was not isolated, and its spectroscopic data are given in Table 1.

X-ray Crystallography. The data collection was performed on a Bruker CCD-1000 diffractometer with Mo Kα (λ = 0.71073 Å) radiation. The final cell constants were calculated from a set of 4620 strong reflections from the actual data collection. The empirical absorption correction was applied by using the program DIFABS.[16] The systematic absences in the diffraction data were consistent for the space groups *Cc* and *C*2/*c*, but only the latter, centrosymmetric space group *C*2/*c* yielded chemically reasonable and computationally stable results of refinement.[17] A successful solution by the direct methods provided most non-hydrogen atoms from the *E*-map. The remaining non-hydrogen atoms were located in an alternating series of least-squares cycles and difference Fourier maps. All non-hydrogen atoms were refined with anisotropic displacement coefficients. All hydrogen atoms were included in the structure factor calculation at idealized positions and were allowed to ride on the neighboring atoms with relative isotropic displacement coefficients. The molecule of the complex occupies an inversion center.

There were one or more severely disordered solvent molecules also present in the asymmetric unit. A significant amount of time was invested in identifying and refining these molecules as hexanes. Bond length restraints were applied to model these molecules, but the resulting isotropic displacement coefficients suggested that the molecules were mobile. In addition, the refinement was computionally unstable. Option

---

(14) Espenson, J. H. *Chemical Kinetics and Reaction Mexhanisms*; McGraw-Hill: New York, 1995.

(15) Barshop, B. A.; Wrenn, C. F.; Frieden, C. *Anal. Biochem.* **1983**, *130*, 134.

(16) Walker, N.; Stuart, D. *Acta Crystallogr.* **1983**, *A39*, 158.

(17) All software and sources of the scattering factors are contained in the SHELXTL (version 5.1) program library (G. Sheldrick, Bruker Analytical X-Ray Systems, Madison, WI).

(18) Spek, A. L. *Acta Crystallogr.* **1990**, *A46*, C34.

SQUEEZE of program PLATON[18] was used to correct the diffraction data for diffuse scattering effects and to identify the solvate molecules. PLATON calculated the upper limit of volume that can be occupied by the solvent to be 1003.9 Å^3, or 17.4% of the unit cell volume. The program calculated 236 electrons in the unit cell for the diffuse species. This approximately corresponds to 1.25 hexane molecules in the asymmetric unit or five hexane molucules in the unit cell (250 electrons). All derived results in the tables (text and Supporting Information) are based on known contents. No data are given for the diffusely scattering solvent molecules. The final least-squares refinement of 271 parameters against 5906 data resulted in residuals R (based on F^2 for $I \geq 2\sigma$) and R_w (based on F^2 for all data) of 0.0347 and 0.1019, respectively.

Product Analysis. A Bruker DRX-400 spectrometer and a Finnigan TSQ-700 GC/LC quadruple mass spectrometer with electrospray were used to identify the imido(methyl)rhenium complexes and the organic amines. The ^{1}H and ^{13}C chemical shifts were measured relative to the residual ^{1}H and ^{13}C resonances in the deuterated solvents, C_6D_5H ($\delta_H = 7.16$ ppm, $\delta_C = 128.39$ ppm), CD_2HCN ($\delta = 1.94$ ppm), and $CD_2HC_6D_5$ ($\delta = 2.09$ ppm).

Results

Reactions with H$_2$O. The compound $CH_3Re(NAd)_3$ (**1a**, Ad = 1-admantyl) is moisture sensitive and gradually reacts with H_2O to give oxorhenium species and $AdNH_2$ according to eq 1. The formation of **2a** and **3a** occurs without the production of side products, whereas the formation of MTO was slow and not clean.[19] Though the kinetics have not been studied hitherto, complexes **1b**−**3b** are known to be moisture sensitive.[11] The rhenium species and RNH_2 were identified by comparing the literature NMR data.[10,11] As shown in Table 1, the chemical shifts of the methyl group bound to rhenium are systematically shifted as the number of imido groups changes.

$$CH_3Re(NR)_3 \xrightarrow[-RNH_2]{+H_2O} CH_3Re(NR)_2O \xrightarrow[-RNH_2]{+H_2O}$$

1a: R = Ad **2**
1b: R = Ar

$$CH_3Re(NR)O_2 \xrightarrow[-RNH_2]{+H_2O} CH_3ReO_3 \quad (1)$$

3 MTO

Reactions with H$_2$S. ^{1}H NMR studies showed that the same rhenium product was produced from the reactions of **1b**/H_2S and **2b**/H_2S. Free $ArNH_2$ (Ar = 2,6-diisopropylphenyl) was observed in the former reaction, while H_2O was produced in the latter one. The intensities of the ^{1}H resonances indicate that this rhenium product incorporates two imido groups for each Re−CH_3 moiety with chemical shifts similar to those of **2b**. X-ray diffraction studies confirmed the rhenium product having a formula of $\{CH_3Re(NAr)_2S\}_2$, see below. To see if a dimer−monomer equilibrium is established in solution, variable temperature NMR studies were carried out in toluene-d_8. The chemical shift of the methyl protons bound to rhenium and that of the isopropyl methine protons on the imido ligands drifted to lower field as the temperature was decreased. Specifically, the chemical shift of Re−CH_3 shifted from 2.38 to 2.46 ppm from 298 to 203 K. Nevertheless, only one signal for Re−CH_3 and one for CH(CH_3)$_2$ were observed in this temperature range.

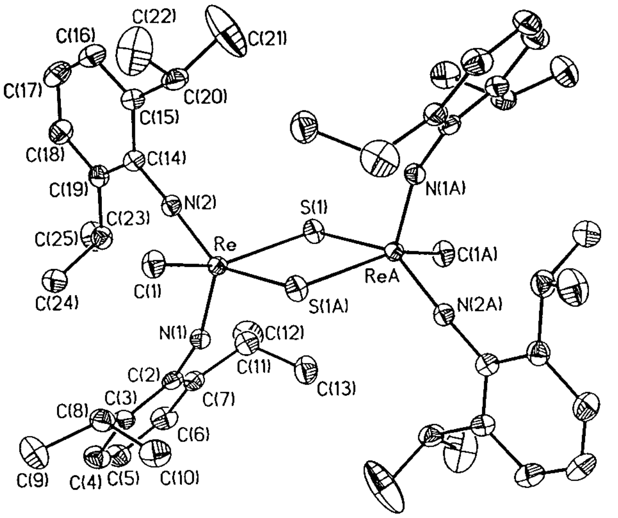

Figure 2. ORTEP view of the crystal structure of $\{CH_3Re(NAr)_2\}_2(\mu\text{-}S)_2$ (Ar = 2,6-diisopropylphenyl) with thermal ellipsoids at the 30% probability level.

Table 2. Crystallographic Data and Selected Bond Lengths (Å) and Bond Angles (deg) for $\{CH_3Re(NAr)_2\}_2(\mu\text{-}S)_2$ (Ar = 2,6-diisopropylphenyl)

chemical formula	$C_{50}H_{74}N_4Re_2S_2$	fw	1167.65
unit cell dimens		cryst syst	monoclinic
a	30.4831(19) Å	space group	$C2/c$
b	10.9766(7) Å	temp	183(2) K
c	18.1645(11) Å	λ	0.71073 Å
α	90°	density (calcd)	1.344 g/cm^3
β	108.268(1)°	abs coeff	42.94 cm^{-1}
γ	90°	R^a	0.0347
vol	5771.5(6) Å^3	$R_w{}^a$	0.1019
Z	4		
Re(1)···Re(A)	3.719	Re(1)−S−Re(A)	102.71(3)
Re(1)−S	2.3448(9)	S−Re(1)−S(A)	77.29(3)
Re(1)−S(A)	2.4171(8)	N(1)−Re(1)−N(2)	113.37(13)
Re(1)−C(1)	2.160(4)	C(1)−Re(1)−N(1)	101.75(13)
Re(1)−N(1)	1.739(3)	C(1)−Re(1)−N(2)	89.22(14)
Re(1)−N(2)	1.750(3)	C(1)−Re(1)−S(1)	144.19(10)
		C(1)−Re(1)−S(A)	77.11(10)
N(1)−Re(1)−S(1)	108.49(10)	Re(1)−N(1)−C(2)	157.6(2)
N(1)−Re(1)−S(A)	104.13(9)	Re(1)−N(2)−C(14)	176.7(3)

[a] $R(wF^2) = \Sigma[w(F_o^2 - F_c^2)]/\Sigma[w(F_o^2)^2]^{1/2}$; $R = \Sigma\Delta/\Sigma(F_o)$, $\Delta = |(F_o - F_c)|$.

The yellow solution of **1a** in C_6D_6 changed to pink upon exposure to H_2S, eq 2. The ^{1}H NMR spectrum indicated that free $AdNH_2$ was produced and the chemical shift for the methyl protons on rhenium shifted from 1.99 to 2.03 ppm. On the basis of the intensities and the structural identification of **4b**, the compound **4a** was suggested to be the product of the hydrosulfidolysis of **1a**. Compared with the ^{13}C chemical shift of 0.80 ppm for $CH_3Re(NAd)_2O$, the chemical shift for $\{CH_3Re(NAd)_2\}_2(\mu\text{-}S)_2$ is 3.9 ppm. A similar downfield shift from 10.5 to 13.8 ppm was observed for **2b** to **4b**.

$$CH_3Re(NR)_3 \xrightarrow[-RNH_2]{+H_2S} CH_3Re(NR)_2S \rightarrow$$

1a: R = Ad **4′**
1b: R = Ar

$$\{CH_3Re(NR)_2\}_2(\mu\text{-}S)_2 \quad (2)$$

4

Crystal Structure of 4b. The molecular structure of **4b** is shown in Figure 2. Selected bond lengths and bond angles are given in Table 2. The dimeric complex contains two five-coordinate rhenium atoms linked by unsymmetrical μ^2-S bridges. The complex occupies a crystallographic inversion center, and hence one half of it is symmetry independent. Each rhenium atom is coordinated to two bridging sulfur atoms, two 2,6-diisopropylphenylimide ligands, and a methyl group. The Re_2S_2 core is planar due to the symmetry considerations. The

---

(19) MTO and perrhenate ion were observed in the hydrolysis of **3b**. See ref 11.

coordination environment about the rhenium is distorted square pyramidal. Atoms S(1), S(1a), N(2), and C(1) are planar within 4 pm and form the basal plane. The rhenium atom is displaced 0.627 Å from this plane. The apical position is occupied by the N(1) atom with the N(1)−Re vector being at 85.7° to the basal plane. The Re−S distances (2.3448(9) and 2.4171(8) Å) are different, but fall in the usual range for this type of Re−S interaction. The Re═N double bonds possess peculiar features. Unexpectedly, the shorter Re−N(1) bond (1.739(3) Å) is observed for the Re−N(1)−C(2) angle of 157.6(2)°, while the longer Re−N(2) distance (1.750(3) Å) corresponds to the much more linear angle Re−N(2)−C(14) spanning 176.7(3)°. This discrepancy may be tentatively attributed to the different nature of the coordination sites occupied by the two ligands. Atom N(1) is in the apical position while atom N(2) occupies an equatorial position. Predictably, the shorter Re−N(1) distance results in the concomitant elongation of the N(1)−C(2) bond distance to 1.387(4) Å as compared to the shorter N(2)−C(14) distance measuring 1.364(5) Å.

Reactions with RNH_2. Complex **1b** (10 mM) did not react with $AdNH_2$ (60 mM) at room temperature in C_6D_6. Neither 2,6-dimethylaniline ($Ar'NH_2$) nor ammonia reacted with $MeRe(NAr)_3$ in 2 days. However, complex **1a** reacts with $Ar'NH_2$ according to eq 3. The ^1H NMR spectrum of an aged (18 h) solution containing 9.0 mM $Ar'NH_2$ and 3.0 mM **1a** in C_6D_6 showed free $AdNH_2$ and two singlets at 2.48 and 2.20 ppm with intensities of 2:1. Over 75% of the starting **1a** had been converted into this new species, which we tentatively assigned as **5a**. The singlet at 2.48 ppm is from the methyl groups of the 2,6-dimethylphenylimido moiety and that at 2.20 ppm from the methyl group on rhenium. Further reaction to produce **6a** was also observed, though only 20% was in that form after 3 days. Free $AdNH_2$ was also formed from the reactions of **1a** with benzylamine, 4-methoxyaniline, and ammonia. These reactions are faster than that of **1a** with 2,6-dimethylaniline, but the corresponding rhenium species was not fully characterized.

$$\underset{\textbf{1a}}{CH_3Re(NAd)_3} \xrightarrow[-RNH_2]{+Ar'NH_2} \underset{\textbf{5a}}{CH_3Re(NAd)_2(NAr')} \xrightarrow[-RNH_2]{+Ar'NH_2} \underset{\textbf{6a}}{CH_3Re(NAd)(NAr')_2} \quad (3)$$

Kinetics. Both the NMR and the UV−vis studies established that the hydrolysis of **1a** in benzene was clean; it was accompanied by an isosbestic point at 352 nm. Though the reaction of **1b** and H_2O in benzene was clean, it was slow. To afford the hydrolysis of **1b** at an experimentally convenient rate a high concentration of H_2O is needed. The moderate solubility of **1b** in acetonitrile and the miscibility of water and acetonitrile allowed us to study the hydrolysis of **1b** in CH_3CN over a wide range of $[H_2O]$. Changing the solvent from CH_3CN to C_6H_6 affects the rate constant only moderately. For example, $k = (1 \pm 0.2) \times 10^{-5}$ L mol^{-1} s^{-1} at 298 K in C_6H_6, compared with $k = (1 \pm 0.2) \times 10^{-4}$ L mol^{-1} s^{-1} at 313 K in CH_3CN. Detailed kinetic analyses are given in the Experimental Section, and the second-order rate constants are summarized in Table 3.

H_2S reacts with **2b** much more rapidly than it does with **1b**. The formation of **4b** was monitored at 575 nm in CH_3CN. Unlike the reaction in C_6H_6, in CH_3CN the reaction is accelerated by Brønsted bases. At constant concentrations of $ArNH_2$ and H_2O, the pseudo-first-order rate constant was first-order with respect to the concentrations of **2b** and H_2S, Figure 3. When the concentrations of **2b** and H_2S were kept constant, the observed rate constant increased linearly as the concentration of $ArNH_2$ increased. Similarly, the rate constant increased when 4-methoxypyridine was added.

Table 3. Second-Order Rate Constants (L mol^{-1} s^{-1}) for Reactions of $CH_3Re(NR)_3$ and $CH_3Re(NR)_2O$ with H_2O and H_2S in C_6H_6 at 298 K

	H_2O	H_2S
$CH_3Re(NAd)_3$	3.3 ± 0.8	17 ± 2
$CH_3Re(NAr)_3$	$(1 \pm 0.2) \times 10^{-4\,a,b}$	$(1.6 \pm 0.3) \times 10^{-4\,a}$
$CH_3Re(NAd)_2O$	$(9 \pm 1) \times 10^{-3}$	95 ± 10
$CH_3Re(NAr)_2O$	$(4 \pm 1) \times 10^{-6\,a,b}$	$(3.3 \pm 0.3) \times 10^{-3\,a,c}$

[a] In CH_3CN. [b] At 313 K. [c] 0.28 L mol^{-1} s^{-1} in the presence of 1.4 mM $ArNH_2$ (see text).

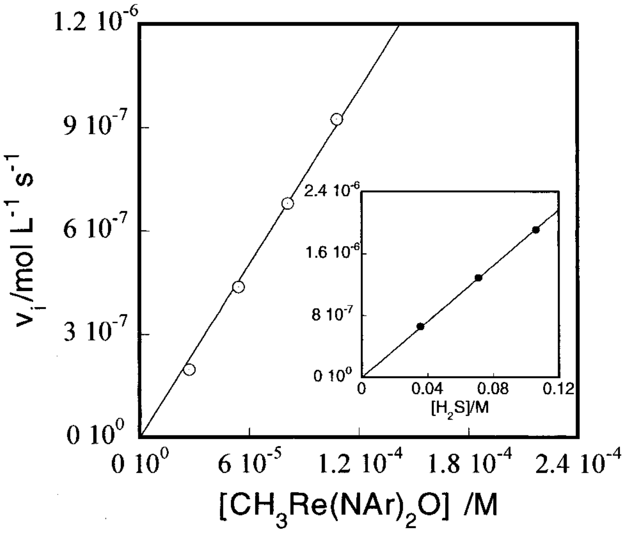

Figure 3. Plot showing that the initial rates (mol L^{-1} s^{-1}) of reaction between $[CH_3Re(NAr)_2O]$ and 1.4 mM $ArNH_2$ and 35 mM H_2S are a linear function of the initial concentration of the rhenium compound. The inset shows the initial rate against $[H_2S]$ with 2.4 mM $ArNH_2$ and 54 μM $CH_3Re(NAr)_2O$. Reactions were carried out in CH_3CN at 298 K.

Discussion

The nature of $CH_3Re(NAr)_nO_{3-n}$ ($n = 1-3$) in solution and in the solid state has been studied by Herrmann and coworkers.[11] The compound **1b** is monomeric in solution as well as in the solid state. On the other hand, both monomeric and dimeric forms exist in solution for complexes **2b** and **3b**, with the monomeric species dominating at room temperature. Like its arylimido analogue, **1a** was shown by crystallographic studies to be a monomer in the solid state.[10] The adamantylimido(oxo)-rhenium species, with less tendency to dimerize owing to the bulk of the NAd unit, may behave similarly to their arylimido analogues in solution.

As its oxo counterpart, the compound **4b** is a dimer in the solid state. Unlike the oxo analogue, however, only one set of the isopropyl methine protons was observed in solutions at 25 to −70 °C, indicating that only one species is probably present in the solution. Spectrophotometric analyses show that absorptions of the sulfido complex in C_6H_6 at 575 nm and other wavelengths obey Beer's law. Furthermore, only two methyl−rhenium resonances are observed in the ^1H NMR spectrum of the mixture of sulfido and oxo complexes, indicating that a possible product, $[CH_3Re(NAr)_2]_2(\mu\text{-}S)(\mu\text{-}O)$, is not formed. These observations suggest the presence of only a single sulfido species in solution; we believe that it is the dimer. One of the reasons that the sulfur-bridged rhenium dimer, **4b**, prefers the dimeric form in both solution and solid, while the oxo-bridged

Scheme 1

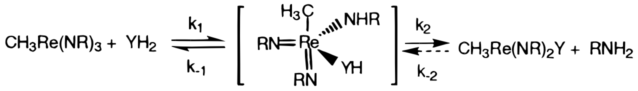

dimer, $\{CH_3Re(NAr)_2\}_2(\mu\text{-}O)_2$, prefers the dimeric form in the solid state but the monomeric form in solution at room temperature is that the Re═O bond is much stronger than the Re═S bond. The strong Re═O double bond may be responsible for the preference of a double bond in **2b** over two single bonds in $\{CH_3Re(NAr)_2\}_2(\mu\text{-}O)_2$ in solution at room temperature. Also, the Re−Re distance in $\{CH_3Re(NAr)_2\}_2(\mu\text{-}O)_2$ is shorter than that in **4b** (312 vs 372 pm). This indicates that the steric interaction between the arylimido ligands on the two rhenium centers is more pronounced in the case of the oxygen derivative. Furthermore, it is known that $(\eta^5\text{-}RC_5H_4)_2Mo{=}O$ with R = Me and *t*-Bu are monomers, whereas the heavier chalcogen derivatives are dimers, $[(\eta^5\text{-}Bu^tC_5H_4)_2Mo]_2(\mu\text{-}Y)_2$ (Y = S, Se, Te).[20]

The reactions of MTO with hydrogen sulfide and dithiols often lead to a reduction of the metal center.[21,22] Isolation of the stable rhenium(VII) sulfido species, **4b**, clearly indicates that the imido ligand is a better electron donor than the oxo ligand, which has also been noted from the ^{17}O chemical shifts in the $CH_3Re(NAr)_nO_{3-n}$ system.[11]

Mechanism. The following mechanism is proposed for the reactions between **1** and H_2Y (Y = O, S, NAr′), Scheme 1. This scheme is analogous to the one proposed for oxygen exchange between CH_3ReO_3 and $H_2{}^{17}O$ or $H_2{}^{18}O$.[23,24] As in the case of that exchange reaction, the intermediate in the $CH_3Re(NR)_3/H_2Y$ reaction was not observed. However, examples of similar intermediates in the hydrolysis of organic imines and aminolysis of ketones are well documented.[25−27] Also, complexes of the type $Cp^*{}_2M(YH)_2$ (M = Ti, Zr; Y = S or O) have been structurally characterized.[28−30] The most convincing evidence comes from the isolation of $(\eta^6\text{-cymene})Os[1,2\text{-}(NH)\text{-}C_6H_4]$ from the reaction of $(\eta^6\text{-cymene})Os(N\text{-}t\text{-}Bu)$ and 1,2-phenylenediamine.[8]

The reverse step of the elimination of amines (k_{-2}) in Scheme 1 is so slow under the experimental conditions that it can be ignored; only a very small amount of amine was generated. Since the intermediate never attained a detectable level, the elimination reactions are likely faster than addition (k_{-1}, $k_2 \gg k_1$). Similar to the mechanism proposed for the aminolysis of imines,[31] this reaction proceeds by rate-controlling nucleophilic attack at the rhenium center. This mechanism is supported by the reactivity order discussed below. Scheme 1 does not include a step leading to **4b** for the H_2S reaction, but the dimerization reaction is believed to be fast. This conclusion is supported by the linear dependence on the initial concentration of **2b**, as shown in Figure 3.

Scheme 2

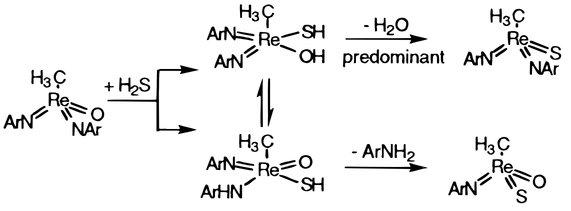

It should be noted that the reaction between **2b** and H_2S did not lead to the formation of $CH_3Re(NAr)(O)(S)$, but produced **4b′** which, was subsequently dimerized, Scheme 2. The driving force here is not that the Re^{VII}═S bond is stronger than the Re^{VII}═O bond. Indeed, the Re═S bond is weaker than the Re═O bond.[21] Rather, the H−O bond energy of H_2O (498 kJ mol^{-1}) greatly exceeds that of H−S (382 kJ mol^{-1}).

Although $CH_3Re(NAr)(O)(S)$ was not observed by NMR, a small amount of $ArNH_2$ was produced during the reaction of **2b** and H_2S, as indicated by the following observations. The formation of **4b** became faster and faster as the identical increments of **2b** were added to a CH_3CN solution containing a large excess of H_2S, even when H_2O was intentionally added to keep $[H_2O]$ constant throughout the reaction. We attribute this to an accelerating effect of the released $ArNH_2$. The effect of base on the H_2S reaction will be discussed below.

Effect of Base. The reaction between **2b** and H_2S in CH_3CN is accelerated by base. The acid−base reaction, eq 4, is likely responsible for the acceleration. Compared with H_2S, HS^- is a better nucleophile; as a result, reaction 5 should be faster than reaction 6. This base effect was not observed in C_6H_6, possibly because reaction 4 is not favored in benzene (The dielectric constants are 2.3 and 35.9 for benzene and acetonitrile, respectively).

$$H_2S + B \rightleftharpoons HS^- + BH^+ \tag{4}$$

$$CH_3Re(NAr)_2O + HS^- \rightarrow CH_3Re(NAr)_2(SH)O^- \tag{5}$$

$$CH_3Re(NAr)_2O + H_2S \rightarrow CH_3Re(NAr)_2(SH)(OH) \tag{6}$$

Reactivity: 1a vs 1b. Compound **1a** is at least 100 times more reactive than its arylimido analogue toward aromatic aldehydes.[10] Following that pattern, **1b** is significantly less reactive than **1a** toward hydrolysis, hydrosulfidolysis, and aminolysis. **1a** is over 4 orders of magnitude more reactive than **1b** toward H_2O and H_2S. The phenolysis of $Mo(NAr)(N\text{-}t\text{-}Bu)R_2$ occurs selectively at the alkylimido moiety.[32] This precedent suggests the same reactivity order between alkylimido and arylimdo groups observed here. It is possible that this different reactivity pattern results from the difference of the polarity of the Re═NAr and Re═NAd bonds and the basicity of the nitrogen atoms.

Also, **2** is less reactive toward hydrolysis than is **1**. The Re═NR moieties of the mixed oxo−imido compounds are the active centers because hydrolysis at the Re═O bond is simply an exchange reaction. The different reactivity far exceeds the statistical factor (2 vs 3); and it may be due to a more favorable free energy change for the first step than the second step of eq 1. Step 1 may be favored by both enthalpy and entropy terms since the first Re═O bond formed in this step is presumably

---

(20) Kuchta, M. C.; Hascall, T.; Parkin, G. *Chem. Commun.* **1998**, 751.
(21) Jacob, J.; Espenson, J. H. *Chem. Commun.* **1999**, 1003.
(22) Takacs, J.; Cook, M. R.; Kiprof, P.; Kuchler, J. G.; Herrmann, W. A. *Organometallics* **1991**, *10*, 316.
(23) Vassell, K. A.; Espenson, J. H. *Inorg. Chem.* **1994**, *33*, 5491.
(24) Espenson, J. H. *Chem. Commun.* **1999**, 479−488.
(25) Poziomek, E. J.; Kramer, D. N.; Fromm, B. W.; Mosher, W. A. *J. Org. Chem.* **1961**, *26*, 423.
(26) Wendhausen, R., Jr.; Zampiron, E.; Vianna, J. F.; Zucco, C.; Rezende, M. C.; Nome, F. *J. Phys. Org. Chem.* **1990**, *3*, 89.
(27) Forlani, L.; Marianucci, E.; Todesco, P. E. *J. Chem. Res., Synop.* **1984**, 126.
(28) Howard, W. A.; Parkin, G. *Organometallics* **1993**, *12*, 2363.
(29) Bottomley, F.; Drummond, D. F.; Egharevba, G. O.; White, P. S. *Organometallics* **1986**, *5*, 1620.
(30) Bortolin, R.; Patel, V.; Munday, I.; Taylor, N. J.; Carty, A. J. *J. Chem. Soc., Chem. Commun.* **1985**, 456.
(31) Koehler, K.; Sandstrom, W.; Cordes, E. H. *J. Am. Chem. Soc.* **1964**, *86*, 2413.
(32) Bell, A.; Clegg, W.; Dyer, P. W.; Elsegood, M. R. J.; Gibson, V. C.; Marshall, E. L. *J. Chem. Soc., Chem. Commun.* **1994**, 2547.

stronger than the second Re═O bond formed in step 2, and the release of steric strain of **1** in step 1 is greater than that of **2** in step 2.

Re═O vs Re═NR. It is difficult to compare the reactivity of Re═O and Re═NR groups toward hydrolysis since the hydrolysis at the Re═O group, an exchange reaction, cannot be monitored by the use of UV−vis spectrophotometers. However, the reactivity between Re═O and Re═NR moieties may be compared in the hydrosulfidolysis reactions, Scheme 2. The reaction of **2** and H_2S preferentially occurs at the Re═O bond as indicated by the formation of **4**. Kinetic data in Table 3 also show that the hydrosulfidolysis of **2** is favored over that of **1** (95 vs 17 L mol^{-1} s^{-1} in the case of R = Ad, and 3.3×10^{-3} vs 1.6×10^{-4} L mol^{-1} s^{-1} in the case of R = Ar). The strong H−O bond of H_2O (498 kJ mol^{-1}), compared with 368 kJ mol^{-1} for the H−N bond,[33] is likely to provide the thermodynamic driving force. It is possible that the attack occurs at the Re═N bond first followed by a proton shift and amine elimination to the most stable product, Scheme 2.

H$_2$Y. The kinetic data indicate that the reactivity of H_2Y toward **1** decreases in the order Y = S > O > NAr′. Since H_2S is a better nucleophile than H_2O,[34] it is not surprising to see the observed reactivity order. On the basis of the reaction conditions one may deduce that H_2S is also more reactive than H_2O toward (Me$_4$taa)Ti═N-*t*-Bu.[5] The reactivity of amines cannot be rationalized solely on the basis of their nucleophilicity because steric effects also play an important role in the aminolysis reactions. It is unfortunate that the reaction between **1a** and NH_3 is not clean and the kinetic information is not available to compare. A substantial steric effect for the amine/imido exchange reaction is also known in the literature. Bergman and co-workers have shown that (η^6-cymene)Os(N-*t*-Bu) can easily be converted to (η^6-cymene)Os(NAr′) (Ar′ = 2,6-dimethylphenyl) by amine exchange. However, the reaction does not occur with the sterically hindered aniline, ArNH$_2$ (Ar = 2,6-diisopropylphenyl).[8] It is also worth noting that the reverse reaction, from arylimide (η^6-cymene)Os(NAr′) to alkylimide (η^6-cymene)Os(N-*t*-Bu), was not observed.[8]

Conclusions

Alkylimido ligands are much more reactive than the arylimido analogues toward nucleophiles, such as H_2S, H_2O, and RNH$_2$. Among the three nucleophiles, H_2S is the most reactive and the aromatic amine the least. The aminolysis reaction favors the transformation from alkylimido to arylimido complexes but showing substantial steric effect. Unlike the remarkable difference in reactivity between Re═NAd and Re═NAr, the differences between H_2S and H_2O toward the Re═NR moiety and between Re═O and Re═NR toward H_2S are noticeable but not extraordinary.

Acknowledgment. This research was supported by a grant from the National Science Foundation. Some experiments were conducted with the use of the facilities of the Ames Laboratory. We thank Dr. Kamel Harrata of the Iowa State University Mass Spectroscopy Laboratory for the electrospray mass data.

Supporting Information Available: Complete tables of crystallographic data and refinement details and figures for the spectrum of **4b** and the base effect on the hydrosulfidolysis of **2b**. This material is available free of charge via the Internet at http://pubs.acs.org.

IC0000956

---

[33] *CRC Handbook of Chemistry and Physics*, 79th ed.; Lide, D. R., Ed.; CRC Press: Boca Raton, 1998.

[34] Barrett, G. C. In *Comprehensive Organic Chemistry*; Stoddart, J. F., Ed.; Pergamon Press: Oxford, 1979; Vol. 3, p 1.